Cross polarization/magic angle spinning ^{13}C n.m.r. study of solid structure and hydrogen bonding of poly(vinyl alcohol) films with different tacticities

Fumitaka Horii*, Shaohua Hu†, Tsukasa Ito, Hisashi Odani and Ryozo Kitamaru‡
Institute for Chemical Research, Kyoto University, Uji, Kyoto 611, Japan

and Shuji Matsuzawa and Kazuo Yamaura
Faculty of Textile Science and Technology, Shinshu University, Ueda, Nagano 386, Japan
(Received 20 May 1991; revised 25 June 1991; accepted 20 July 1991)

Cross polarization/magic angle spinning (CP/MAS) ^{13}C n.m.r. measurements have been performed at room temperature for poly(vinyl alcohol) (PVA) films with different tacticities to obtain information about the structure and hydrogen bonding in the crystalline and non-crystalline regions. ^{13}C spin-lattice relaxation analyses have revealed that three components exist for each sample, with different spin-lattice relaxation times T_{1C}, which are assignable to the crystalline, less disordered non-crystalline and amorphous components. Using such differences in T_{1C}, we separately recorded the spectra of the crystalline and non-crystalline components, and then analysed the triplets of the CH resonance lines appearing in both spectra in terms of three Gaussians which should be ascribed to CH carbons associated with two, one and no intramolecular hydrogen bond(s) in the *mm*, *mr* and *rr* sequences. As a result, it has been found that the relative intensities of the triplets are not in accord with the contents of the triad sequences, suggesting the formation of intramolecular and intermolecular hydrogen bonds in the *meso* sequences at almost equal probability. The effects of water on hydrogen bonding have also been examined for the almost atactic PVA sample.

(Keywords: solid structure; hydrogen bonding; poly(vinyl alcohol); CP/MAS ^{13}C n.m.r.; spin-lattice relaxation times; effects of water)

INTRODUCTION

Poly(vinyl alcohol) (PVA), which is highly crystalline even in atactic form and hydrophilic due to OH groups, has recently been receiving much attention as a possible raw material for hydrogels and high-tenacity fibres. However, it is very important, in developing such materials, to characterize intramolecular and intermolecular hydrogen bonding in detail. Hydrogen bonding of PVA was previously investigated[1–4] by i.r. spectroscopy using the absorption band at about 3000 cm^{-1} ascribed to the OH stretching or its overtone at about 6700 cm^{-1}. In particular, the latter absorption band was resolved into three lines which were assigned to the OH groups associated with intramolecular, intermolecular and no hydrogen bonding in the order of increasing wavenumber. However, it may be difficult to further resolve these absorption bands into the contributions from the crystalline and non-crystalline regions in such i.r. spectroscopy.

High resolution solid state ^{13}C n.m.r. spectroscopy is very powerful in characterizing the structure of the crystalline and non-crystalline regions of solid polymers[5]. In recent studies, some resonance lines have been resolved into the crystalline and non-crystalline components for polyethylene[6,7], polypropylene[8], poly(tetramethylene oxide)[9] and cellulose[10–13], and therefore the detailed structure and molecular motion are well characterized for the crystalline and non-crystalline regions. In the case of solid PVA, the CH resonance line of the cross polarization/magic angle spinning (CP/MAS) ^{13}C n.m.r. spectrum splits into a triplet, due to the difference in the number of intramolecular hydrogen bonds formed in the *mm* and *mr* triad sequences[14,15]. Using this phenomenon, it is expected that much information may be obtained about the intramolecular hydrogen bonding as well as intermolecular hydrogen bonding in both crystalline and non-crystalline regions for different PVA samples.

In this paper, we first examine the contributions from the crystalline and non-crystalline regions in the CP and ^{13}C spin-lattice relaxation processes at room temperature for PVA films with different tacticities by CP/MAS ^{13}C n.m.r. spectroscopy, which was not fully examined for well-crystallized samples in the previous report[14]. On the basis of these results, we separately record the spectra of

* To whom correspondence should be addressed
† On leave from Shanghai College of Petrochemical Technology, Jinshanwei, People's Republic of China
‡ Present address: Faculty of Science and Technology, Ryukoku University, Seta, Otsu 520, Japan

0032-3861/92/112299-08

the crystalline and non-crystalline components and discuss the structure and hydrogen bonds in these regions. Moreover, the effect of water on hydrogen bonding is also briefly examined for an almost atactic PVA sample. Similar analyses for PVA single crystals and fibres will be published in future papers.

EXPERIMENTAL

Samples

Three types of PVA samples with different tacticities were used. Highly syndiotactic PVA (S-PVA) was prepared by the ammonolysis of poly(vinyl trifluoroacetate), which was polymerized at 60°C at the bulk using benzoyl peroxide as an initiator, in diethylenetriamine[16]. Highly isotactic PVA (I-PVA) was obtained by the debenzylation of poly(benzyl vinyl ether) which was polymerized at −78°C in toluene/hexane (15/5 vol. ratio) using BF_3 etherate as an initiator[17]. Conventional PVA (A-PVA), which was provided by Kuraray Co. Ltd, was purified by complete hydrolysis followed by Soxhlet extraction with methanol. *Table 1* shows viscosity-average degrees of polymerization and triad and dyad tacticities determined at 50°C in deuterated dimethyl sulphoxide by gated scalar decoupling ^{13}C n.m.r. spectroscopy.

Films with a thickness of about 100 μm were prepared by casting aqueous solutions of these PVA samples and then drying at 50°C for about 2 days in vacuum. These films were subjected to annealing for 10 min in an argon atmosphere to avoid an annealing effect during n.m.r. measurements. The annealing temperature was 180°C for A-PVA and S-PVA, and 150°C for I-PVA. Each annealed sample was dried at 50°C for a few days in vacuum, packed into a MAS rotor with an O-ring seal (described later) and further dried at 50°C for 2 days in vacuum. These samples are termed dry PVA samples in this work. On the other hand, some samples were exposed to atmospheres of different relative humidities at 24°C in a desiccator for about 1 week to attain the equilibrium state. These hydrated samples were packed into the MAS rotor and allowed to equilibrate in the same atmospheres for a few more days. The water content is expressed as (g of H_2O/g of dry PVA) × 100%.

^{13}C n.m.r. measurements

High resolution solid state ^{13}C n.m.r. measurements were performed at room temperature on a Jeol JNM-FX200 n.m.r. spectrometer, operating at a static magnetic field of 4.7 T, equipped with a variable temperature (VT)/MAS system. ^1H and ^{13}C radiofrequency field strengths, $\gamma B_1/2\pi$, were 69.4 kHz for the CP process and other pulse sequences used in this work, except for the dipolar decoupling process where the ^1H field strength was reduced to 59 kHz. The contact time for the CP process was 1 ms and the recycle time after collection of the free induction decay (f.i.d.) was 15 s. A cylinder-type MAS rotor with an O-ring seal[10,13], which is shown schematically in *Figure 1* together with a conventional MAS rotor, was used for both dry and hydrated samples to prevent the absorption of moisture or the loss of water by high centrifugation during n.m.r. measurements. The main parts of these MAS rotors are made of aluminium oxide or zirconia and poly(amide imide) resins. The MAS rate was about 3.5 kHz. ^{13}C chemical shifts relative to tetramethylsilane (Me_4Si) were determined by using the CH_2 line at 32.89 ppm of the orthorhombic crystalline component of polyethylene as an internal or external reference.

Table 1 Degrees of polymerization (DP) and tacticities for different PVA samples

Sample	DP	Triad tacticity			Dyad tacticity[a]	
		mm	*mr*	*rr*	*m*	*r*
S-PVA	1590	0.19	0.48	0.33	0.43	0.57
A-PVA	1700	0.23	0.50	0.27	0.48	0.52
I-PVA	300	0.57	0.35	0.08	0.76	0.24

[a]Calculated by the least-squares method assuming Bernoullian statistics

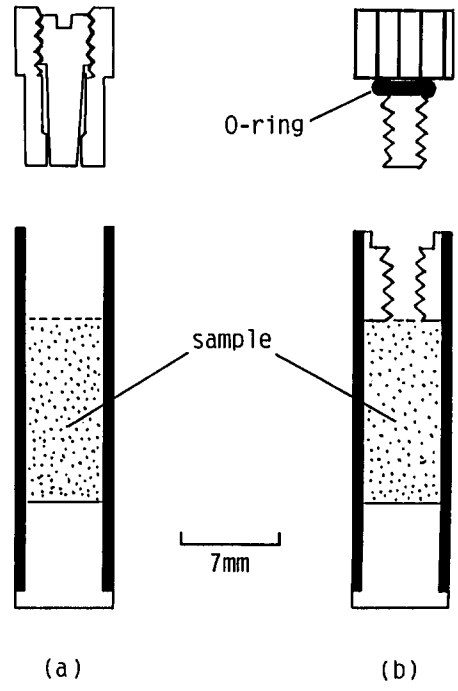

Figure 1 Schematic diagrams of (a) a conventional MAS rotor and (b) a MAS rotor with an O-ring seal

RESULTS AND DISCUSSION

CP/MAS ^{13}C n.m.r. spectra

Figure 2 shows 50 MHz CP/MAS ^{13}C n.m.r. spectra measured at room temperature for dry PVA samples with different tacticities. For comparison, a stick-type scalar-decoupled ^{13}C n.m.r. spectrum of A-PVA in D_2O solution is also shown. The CH resonance line of each sample splits into a triplet, I, II and III, and the splitting is much enhanced in width compared to the case of the triplet ascribed to the CH carbons in the triad sequences *mm*, *mr* and *rr* for the solution state spectrum[18,19].

According to previous work of Terao *et al.*[14], lines I, II and III are assigned to central CH carbons I, II and III in *mm*, *mr* and *rr* sequences of the PVA chain with planar zigzag structure, as shown in *Figure 3*. Here, the OH group bonded to the CH carbon I forms intramolecular hydrogen bonds with two OH groups on both sides in the *mm* sequence. In contrast, the corresponding OH groups associated with CH carbons II and III form one and no intramolecular hydrogen bonds with the

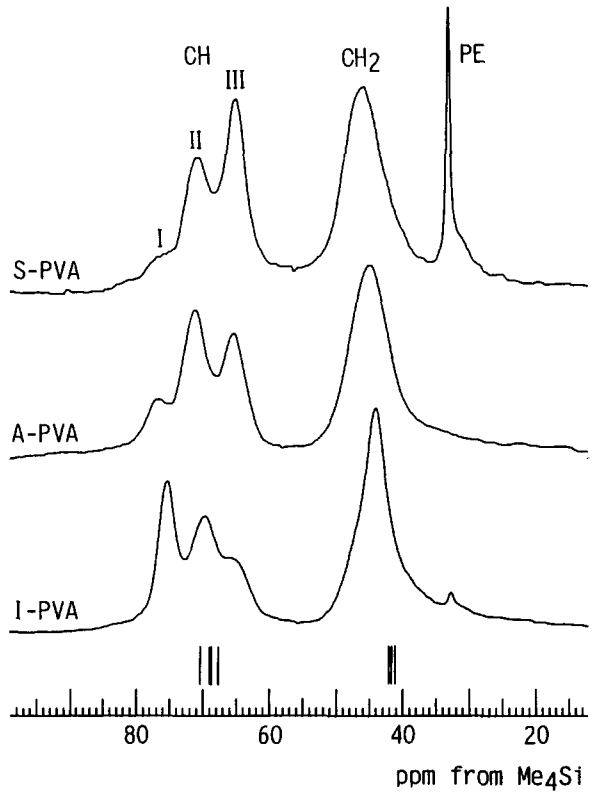

Figure 2 50 MHz CP/MAS ^{13}C n.m.r. spectra of different dry PVA samples measured at room temperature. PE indicates the CH_2 resonance line of the orthorhombic crystalline component of polyethylene inserted as an internal reference

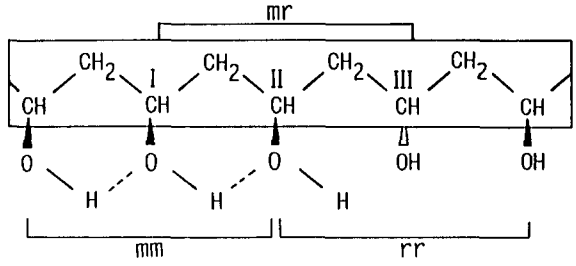

Figure 3 Schematic diagram for intramolecular hydrogen bonding in the triad sequences of PVA

neighbouring OH groups in *mr* and *rr* sequences, respectively. Since the O···O distance is 2.52 Å[20,21] in this intramolecular hydrogen bonding, strong deshielding should occur for the CH carbons I and II, in analogy with the case of hydroxybenzaldehydes[22]. In these crystals, marked downfield shifts appear for the carbons chemically bonded OH groups with decreasing O···O distance, when this distance is less than 2.7 Å in the intramolecular hydrogen bonding between the hydroxyl and carbonyl groups. Accordingly, the most prominent downfield shift should be observed for the CH carbon I of PVA, whereas the second level downfield shift may appear for the CH carbon II. As for the CH carbon III, there is the possibility of intermolecular hydrogen bonding associated with the nearest chains. However, this type of hydrogen bonding will induce almost no downfield shift of the CH carbon III, because the O···O distance is so large (>2.7 Å) for PVA[20,21]. As a result, resonance lines of the CH carbons I, II and III should appear in the order of increasing field, as seen in *Figure 2*.

On the other hand, Ketels *et al.*[23] recently reported another model to explain a similar splitting of the CH carbon resonance observed for solid ethylene–vinyl alcohol copolymers. In this model they considered only the effects of the substitution of OH groups along the methylene sequence, including effects of tacticity and sequence distribution. Although their model is also applicable to the case of PVA, they could not conclude which effect is most important: hydrogen bonding or substitution. Since it has been confirmed by i.r. spectroscopy, as described in the Introduction, that intramolecular hydrogen bonds exist in solid PVA[4], we adopt the assignment proposed by Terao *et al.*[14]. It will also be confirmed by separate CP/MAS ^{13}C n.m.r. experiments[24,25] for different PVA samples at different temperatures that this assignment is most plausible.

As is clearly seen in *Figure 2*, the intensity of line I markedly increases with increasing *mm* content and line III inversely reduces in intensity. These changes seem to be well understood by the above-mentioned assignment. Nevertheless, the relative intensities of lines I, II and III are not in accord with the fractions of *mm*, *mr* and *rr* sequences shown in *Table 1*, as also found in the previous work[14]. For example, the relative intensity ratio of lines I, II and III apparently deviates from 1:2:1 for A-PVA, which is almost atactic. To elucidate the cause of this discordance it is very important to separate the contributions from the crystalline and non-crystalline regions, which was not considered in previous work[14,23]. To this end, we have examined the CP process and ^{13}C spin-lattice relaxation process for the PVA samples at room temperature.

Cross polarization process

In the conventional CP process under Hartmann–Hahn conditions, ^{1}H and ^{13}C spin systems are spin-locked in the rotating frames and thermally contact each other, thus exchanging their energies. The respective spin systems also exchange energies with the surrounding thermal reservoir, the so-called lattice. According to the simple theory[26–29] in this CP process, ^{13}C magnetization, $M_C(t)$, is expressed as a function of the contact time t as follows:

$$M_C(t) = (M_e/T_{CH})(1/T^*_{1\rho C} - 1/T_{1\rho H})^{-1} \times [\exp(-t/T_{1\rho H}) - \exp(-t/T^*_{1\rho C}) \quad (1)$$

$$1/T^*_{1\rho C} = 1/T_{1\rho C} + 1/T_{CH} \quad (2)$$

Here, M_e is the ^{13}C equilibrium magnetization obtained when both spin systems fully contact each other without any energy exchange with the lattice and therefore this value is proportional to the concentration of a given ^{13}C nucleus in a material. T_{CH} is the time constant for the energy exchange between ^{1}H and ^{13}C spin systems, and $T_{1\rho H}$ and $T_{1\rho C}$ are the spin-lattice relaxation times in their rotating frames. When the ^{13}C magnetization is observed by the CP technique, T_{CH} should be much shorter than $T_{1\rho C}$ and $T_{1\rho H}$. Under this condition equation (1) reduces to:

$$M_C(t) = M_e[\exp(-t/T_{1\rho H}) - \exp(-t/T_{CH})] \quad (3)$$

According to this equation, the ^{13}C magnetization appears at the rate of the order of $(T_{CH})^{-1}$ and disappears at the rate of $(T_{1\rho C})^{-1}$.

Figure 4 shows a semilogarithmic plot of the peak intensity as a function of the contact time t for the CH

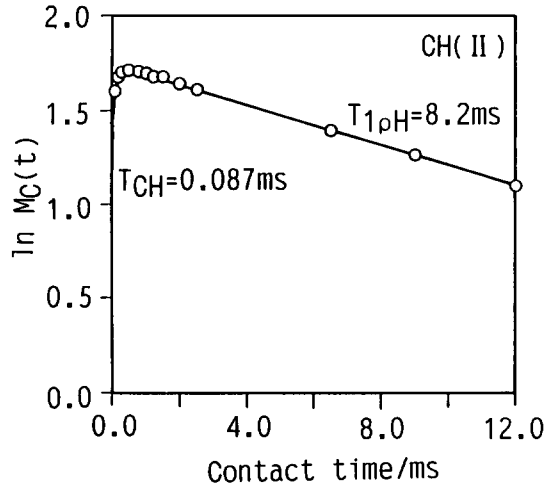

Figure 4 CP process for the resonance line of CH carbon II of A-PVA measured at room temperature. The solid curve is the result calculated by equation (3)

Table 2 Time constants (T_{CH}) for the energy exchange between ^1H and ^{13}C spin systems and ^1H spin-lattice relaxation times ($T_{1\rho H}$) in the rotating frame measured at room temperature for A-PVA

Resonance line	T_{CH} (ms)	$T_{1\rho H}$ (ms)
I	0.083	8.2
II	0.087	8.2
III	0.092	7.8
CH_2	0.070	8.6

line II of A-PVA. The solid curve indicates the theoretical result based on equation (3) obtained by a computer least-squares method. The experimental data are in good accord with the theoretical curve. Similar good accordance could be obtained for the other lines of A-PVA, and the T_{CH} and $T_{1\rho H}$ values thus obtained are listed in *Table 2*. Although this sample is composed of the crystalline and non-crystalline regions, the respective resonances give single T_{CH} and $T_{1\rho H}$ values. Therefore, it seems impossible to separately record the spectra of the crystalline and non-crystalline components using an appropriate contact time in the CP process.

It should, however, be noted that the $T_{1\rho H}$ values of the respective lines are in good accord with each other. This suggests that ^1H spins fully diffuse between the crystalline and non-crystalline regions, with the result that this system can be regarded as a homogeneous ^1H spin system. In such a system equation (3) will hold for each ^{13}C nucleus and thus the integrated intensity of each resonance line should be proportional to the real concentration of the corresponding ^{13}C nucleus, which corresponds to $M_e \exp(-t/T_{1\rho H})$, in spectra obtained by setting $t \geqq 5T_{CH}$. In fact, the ratio of the integrated intensities of the CH and CH_2 resonance lines is almost 1:1 for the spectra shown in *Figure 2*. Moreover, a fully relaxed spectrum obtained for A-PVA by a 45° single pulse sequence, where the intensity of each resonance line exactly reflects the concentration of the corresponding ^{13}C nucleus, was almost the same as the CP/MAS ^{13}C spectrum shown in *Figure 2*.

^{13}C spin-lattice relaxation

Figure 5 shows partially relaxed ^{13}C n.m.r. spectra of A-PVA measured at room temperature by CPT1 pulse sequence developed by Torchia[30], where t is the decay time for the spin-lattice relaxation. In *Figure 6* the logarithmic peak intensity of the CH carbon II is plotted against the decay time t (open circles). Here, the contributions from the materials used for the MAS rotor and the probe were removed in determining peak intensities by subtracting spectra obtained by blank measurements from the spectra shown in *Figure 5*.

The decay curve shown in *Figure 6* appears not to be described as a single exponential. The solid line is the decay obtained by the least-squares method, assuming

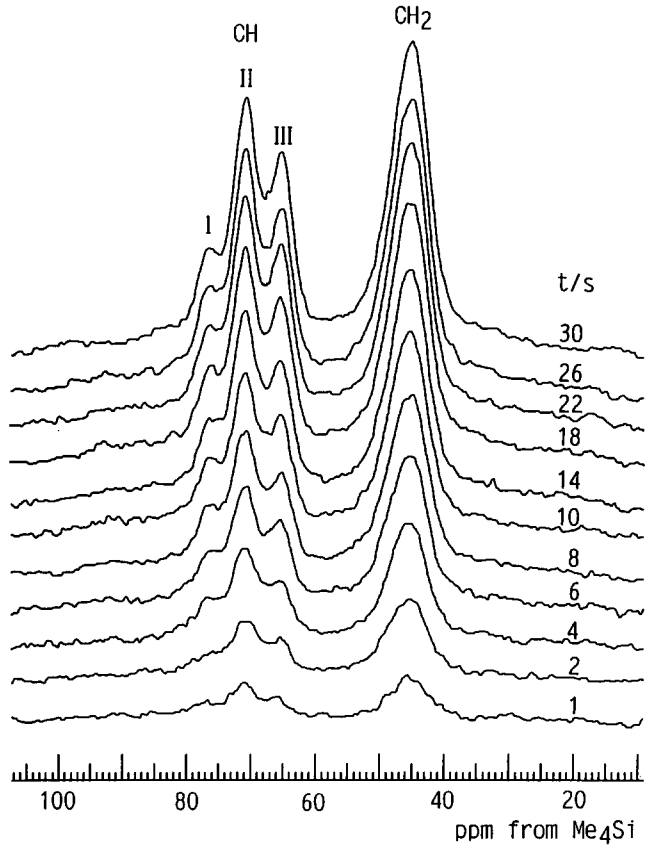

Figure 5 Partially relaxed ^{13}C n.m.r. spectra of A-PVA measured at room temperature by CPT1 pulse sequence

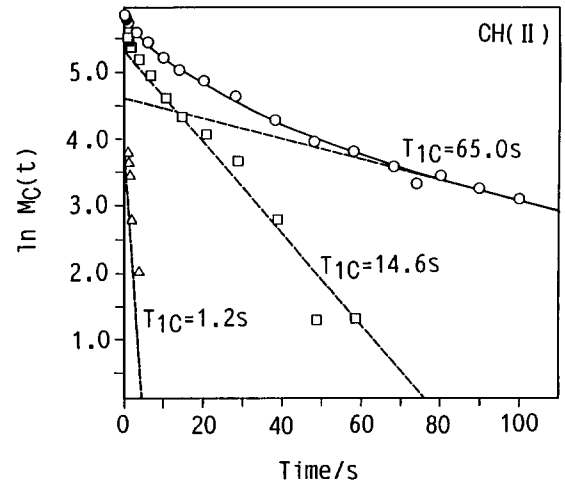

Figure 6 Semilogarithmic plot of the peak intensity of the resonance line of CH carbon II shown in *Figure 5* as a function of time. The solid line is the composite decay curve for the three components with different T_{1C} values, which are shown by broken lines

Table 3 ^{13}C spin-lattice relaxation times of the respective resonance lines of different dry PVA samples, measured at room temperature

Sample	T_{1C} (s)			
	I	II	III	CH_2
S-PVA	74.2, 13.2, n.m.	58.3, 8.7, n.m.	89.5, 12.3, n.m.	71.1, 9.2, n.m.
A-PVA	60.0, 12.1, 1.1	65.0, 14.6, 1.2	62.0, 12.3, 2.2	65.0, 14.6, 1.3
I-PVA	51.3, 10.4, n.m.	39.7, 7.3, n.m.	32.9, 4.6, n.m.	43.0, 7.8, n.m.

n.m., not measured

three components with different ^{13}C spin-lattice relaxation times, T_{1C}, and the decays of these three componens are also shown as broken lines. The experimental points agree well with the calculated curve, indicating that three components exist with different T_{1C} values. Similar three-component analyses could be performed for other resonance lines of A-PVA. In addition, these three components were also confirmed by the saturation-recovery method modified for solid measurements.

Table 3 lists T_{1C} values of the respective resonance lines of different PVA samples obtained by the CPT1 pulse sequence. Here, only the longer two T_{1C} values were measured for S-PVA and I-PVA, although similar shortest T_{1C} components were confirmed for these samples. Since the glass transition temperature[31] of dry A-PVA is about 70°C or about 85°C, the molecular motion of PVA chains must be restricted at room temperature. Under this situation the longer T_{1C} value should indicate less mobility for components in a sample. Accordingly, the component with T_{1C} values of 33–90 s can be assigned to the crystalline component, because this component is most rigid at room temperature. Moreover, a similar three-component analysis of the decay curve, expressed as integrated intensity for the CH_2 line of A-PVA shown in *Figure 5*, gave the fractions of the three components: 0.38, 0.42 and 0.20 for the components with T_{1C} values of 65.0, 14.6 and 1.3 s, respectively. The fraction thus obtained for the longest T_{1C} component is in good accord with the degree of crystallinity (0.42) determined from the heat of fusion by d.s.c., where the heat of fusion for the PVA crystals was assumed[32] to be 6.99 kJ mol^{-1}. This fact therefore confirms the above assignment and also allows us to assign the other two components to the non-crystalline component. A more detailed assignment of the latter two components is not easy at present, but since the shortest T_{1C} component is more mobile compared to the non-crystalline component with longer T_{1C} values, this component may be assigned to the amorphous component. This assignment is supported by the fact that the rubbery component appears as a result of the disappearance of the shortest T_{1C} component when water is added to A-PVA, as will be described later, or when the temperature is increased above T_g (ref. 24). In addition, the other non-crystalline component may therefore be ascribed to the less disordered component, located in the interfacial region between the crystalline and amorphous regions as in the cases of other crystalline polymers[6–9].

Spectra of the crystalline and non-crystalline components

As described above, the T_{1C} values of the crystalline components are more than about 5 times larger than the values of the non-crystalline components. Using this difference in T_{1C}, the spectra of the two components are separately recorded in the following way. When resonance line j on a conventional CP/MAS ^{13}C n.m.r. spectrum contains the crystalline and non-crystalline components, the intensity M_j^{CP} may be expressed as a sum of the two contributions M_{jC} and M_{jNC} as follows:

$$M_j^{CP} = M_{jC} + M_{jNC} \quad (4)$$

On the other hand, the intensity $M_j(t)$ of resonance line j measured at time t by the CPT1 pulse sequence will be given by:

$$M_j(t) = M_{jC}(0)\exp(-t/T_{1jC}) + M_{jNL}(0)\exp(-t/T_{1jNL}) + M_{jNS}(0)\exp(-t/T_{1jNS}) \quad (5)$$

Here, $M_{jC}(0)$, $M_{jNL}(0)$ and $M_{jNS}(0)$ are the intensities of the crystalline component and the non-crystalline components with the long and short T_{1C} values for resonance line j, respectively, and T_{1C}, T_{1NL} and T_{1NS} are the ^{13}C spin-lattice relaxation times of the corresponding components. When the spectrum is measured by the CPT1 pulse sequence under the conditions $t \geqslant 5T_{1jNL}$, it reflects the crystalline component with the intensities

$$M_{jC}(t) = M_{jC}(0)\exp(-t/T_{1jC}) \quad (6)$$

as a result of the disappearance of all the non-crystalline components. As an example, *Figure 7b* shows the spectrum of the crystalline components of A-PVA measured at $t = 49.9$ s. Since the T_{1C} values of the respective lines differ somewhat from each other, as

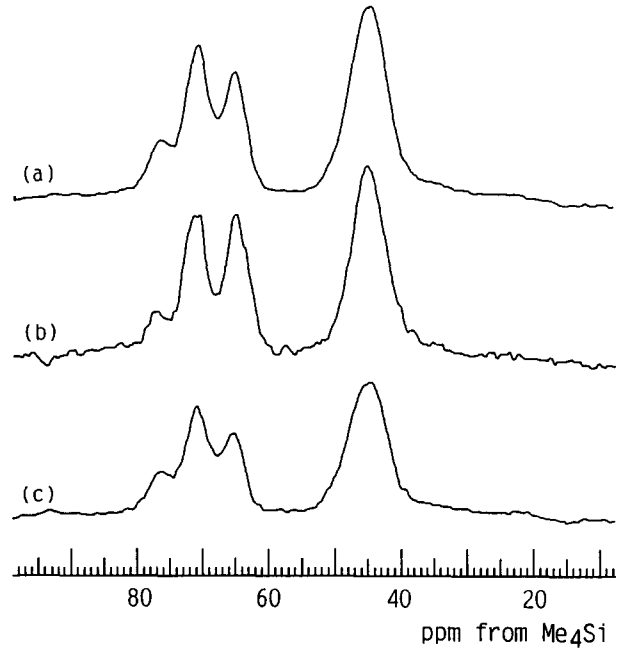

Figure 7 CP/MAS ^{13}C n.m.r. spectra of different components of A-PVA: (a) total; (b) crystalline; (c) non-crystalline ((a) − 0.29(b))

shown in *Table 3*, the relative intensities of these lines are in disaccord with those of the unrelaxed spectrum. The correction of the relative intensities will be described later.

The spectrum of the non-crystalline component can be obtained by subtracting the crystalline spectrum (*Figure 7b*) from the total CP/MAS ^{13}C n.m.r. spectrum (*Figure 7a*). However, it is not as simple to conduct such subtraction for the spectra of PVA, unlike the case of native cellulose[10–13,29], because the respective spectra of these components are completely superposed on each other. In this study we first determined the values $M_{jC}(0)$, $M_{jNL}(0)$ and $M_{jNS}(0)$ by the T_{1C} analysis based on equation (5) and then carried out the subtraction to obtain the following peak intensity ratio of the crystalline and non-crystalline components for line II:

$$M_{jC}/M_{jNC} = M_{jC}(0)/[M_{jNL}(0) + M_{jNS}(0)] \quad (7)$$

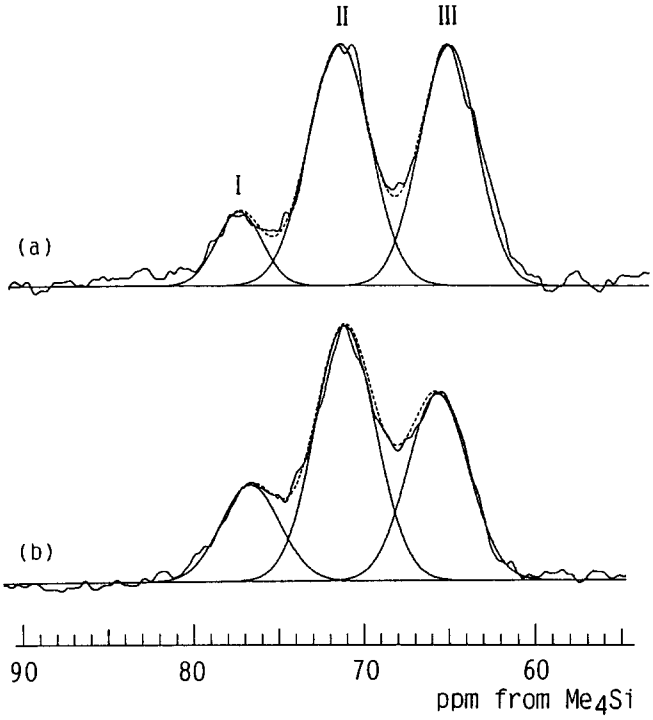

Figure 8 Lineshape analysis for the CH lines of (a) crystalline and (b) non-crystalline components of A-PVA. The broken line indicates the composite curve of the three components shown by solid lines

Figure 7c shows the spectrum thus obtained for the non-crystalline component of A-PVA. The correction of the exact relative intensity of this spectrum will also be described later.

Figure 8 shows the results of the computer lineshape analysis for the CH resonance lines of the crystalline and non-crystalline components of A-PVA, which correspond to *Figures 7b* and *7c*, respectively. Here, each line was assumed to be described as Gaussian. The composite curve of the three lines I, II and III, which is shown by a broken line, is in good agreement with the experimental spectrum for both crystalline and non-crystalline components. The integrated fractions of lines I, II and III obtained by this analysis are given in *Table 4*, together with their ^{13}C chemical shifts and linewidths. Similar analytical results are also shown in this table for the crystalline component of S-PVA and I-PVA. As already described, the fractions obtained from the spectra corresponding to *Figures 7b* and *7c* include the effect of the difference in T_{1C} among the CH carbons. As for the crystalline component, the fractions were corrected according to equation (6) using T_{1C} values shown in *Table 3*. On the other hand, the correction of the fractions for the non-crystalline spectrum was made by multiplying the fraction of line j by factor g_j, which is expressed as:

$$g_j = M_j^{CP}/(1 + f_j)M_{jNC'}(t) \quad (8)$$

and then normalizing those values. Here, M_j^{CP} and $M_{jNC'}(t)$ are the peak intensities of line j for the spectra shown in *Figures 7a* and *7c*, and f_j is the peak intensity ratio for the crystalline and non-crystalline components of line j, which is given by equation (7).

As is clearly seen in *Table 4*, the corrected fractions of the respective CH lines of the crystalline component are still in disaccord with the fractions of the triad tacticities shown in *Table 1* for each PVA sample. This may be because all OH groups in the *meso* sequences do not form intramolecular hydrogen bonds and some of them are associated with the intermolecular hydrogen bonding. In fact we estimated the approximate fractions of lines I, II and III assuming that intramolecular and intermolecular hydrogen bonds are formed at equal probability in the *meso* sequences[33]. In this case it was assumed that the intermolecular hydrogen bonding does not induce any downfield shift. Therefore, line I was ascribed purely to the CH carbons associated with the two intramolecular

Table 4 Integrated fractions, chemical shifts and linewidths of lines I, II and III of CH carbons for the crystalline and non-crystalline spectra of different dry PVA samples

	Integrated fraction			Chemical shift (ppm)			Linewidth (Hz)		
Sample	I	II	III	I	II	III	I	II	III
Crystalline									
S-PVA observed	0.080	0.349	0.571	76.7	71.1	64.9	193	201	156
corrected[a]	0.064	0.350	0.586						
A-PVA observed	0.105	0.467	0.428	77.0	71.2	64.8	156	214	197
corrected[a]	0.109	0.457	0.434						
I-PVA observed	0.481	0.329	0.190	75.4	69.8	64.7	141	237	211
corrected[a]	0.386	0.351	0.263						
Non-crystalline									
A-PVA observed	0.175	0.477	0.348	76.5	70.9	65.5	203	211	209
corrected[b]	0.170	0.493	0.337						

[a]Corrected by equation (6)
[b]Corrected by equation (8)

hydrogen bonds in some of the *mm* sequences. However, additional contributions appear for lines II and III: CH carbons forming one intramolecular hydrogen bond in the *mm* sequences in addition to those in *mr* sequences for line II and CH carbons associated with no intramolecular hydrogen bonding in the *mm* and *mr* sequences as well as in the *rr* sequence for line III. As a result, the fractions thus calculated agreed quite well with the corrected fractions shown in *Table 3* for the crystalline components of the different PVA samples. More detailed calculation[34] is in progress but the preliminary calculation fully revealed that the intramolecular and intermolecular hydrogen bonds are formed at nearly equal probability in the *meso* sequences, and this leads to the marked difference between the fractions of lines I, II and III and the contents of *mm*, *mr* and *rr* sequences.

On the other hand, the chemical shifts and the linewidths of the non-crystalline CH lines for A-PVA, which are shown in *Table 4*, are almost the same as those of the crystalline components for A-PVA as well as S-PVA and I-PVA. Moreover, the fractions of the CH lines of the non-crystalline component do not greatly differ from those of the crystalline component for A-PVA. These results suggest that no marked difference in structure exists between the crystalline and non-crystalline regions, as judged from the hydrogen bonding in the triad sequences. Nevertheless, slight increases in fraction for lines I and II probably indicate that the intramolecular hydrogen bonds are somewhat preferentially formed in the non-crystalline region.

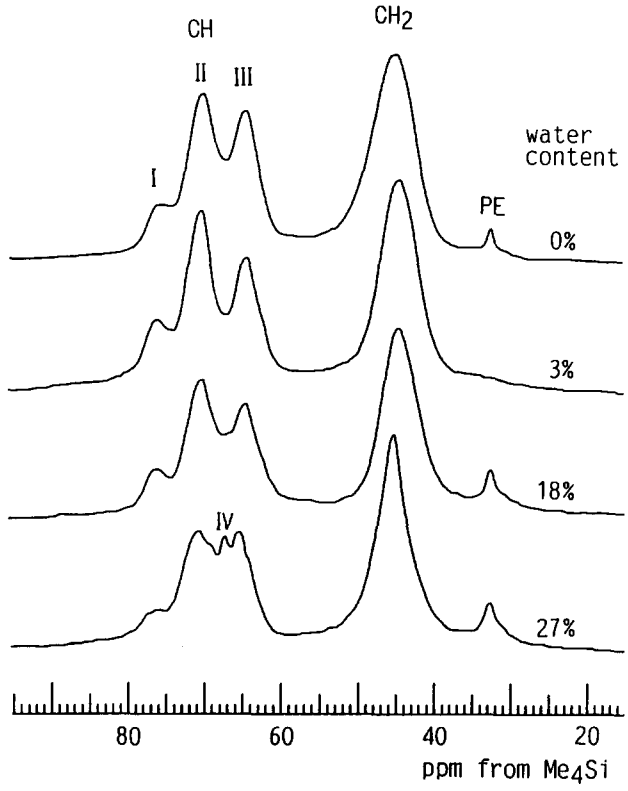

Figure 9 50 MHz CP/MAS ^{13}C n.m.r. spectra of A-PVA with different water contents

Structure in the hydrated state

Figure 9 shows CP/MAS ^{13}C n.m.r. spectra of A-PVA with different water contents. An additional resonance line, which is termed line IV, appears between lines II and III for samples with a water content greater than 18%. *Table 5* shows T_{1C} values of the respective resonance lines of A-PVA with different water contents, which were measured by CPT1 pulse sequence. It is evident that three components exist with different T_{1C} values for A-PVA with a water content of 18%. The shortest T_{1C} component, which corresponds to line IV, may be assigned to the rubbery component where the intramolecular and intermolecular hydrogen bonds are broken by water molecules.

In order to confirm this assignment, we measured the ^{13}C spin-spin relaxation process for A-PVA with a water content of 18%. As a result, line IV was still observed at a decay time t of more than 100 μs, whereas all contributions from lines I, II and III disappeared at shorter values of t. *Figure 10* shows the spectrum measured at $t = 200$ μs at room temperature together with the pulse sequence used for the ^{13}C spin-spin relaxation measurement. For comparison, the spectrum measured at 90°C by the same pulse sequence is also shown in this figure. In both spectra a larger splitting due to lines I, II and III is not observed in the CH resonance line. In contrast, a finer triplet appears, which may be due to the CH carbons in the *mm*, *mr* and *rr* sequences in accord with the solution-state spectrum. It should therefore be concluded that line IV is assigned to the rubbery component. In addition, the components with T_{1C} values of 42–48 s and 5.5–8.5 s can be assigned to the crystalline and less disordered non-crystalline components, although these T_{1C} values are significantly decreased by the absorption of water.

Figure 11 shows the result of the lineshape analysis for the spectrum of the crystalline component of A-PVA with a water content of 18%, which was carried out in the same way as for dry PVA samples. Although an additional Gaussian curve must be introduced upfield for line III, the composite curve of the four lines, which is described by a broken line, reproduces well the experimental spectrum of the crystalline component. The assignment of the additional upfield component is not easy at present. As described in the Introduction, previous i.r. spectroscopy[4] has confirmed that OH groups free from any hydrogen bonding exist together

Table 5 ^{13}C spin-lattice relaxation times of the respective carbons of PVA films with different water contents

Water content (%)	T_{1C} (s)			
	I	II	III	CH_2
0	60.0, 12.1, 1.1	65.0, 14.6, 1.2	62.0, 12.3, 2.2	65.0, 14.6, 1.3
3	60.6, 5.8, n.m.	52.8, 7.0, n.m.	50.1, 6.8, n.m.	51.7, 6.2, n.m.
18	43.7, 8.5, 0.29	42.3, 5.5, 0.25	48.0, 5.5, 0.24	45.6, 6.4, 0.14

n.m., not measured

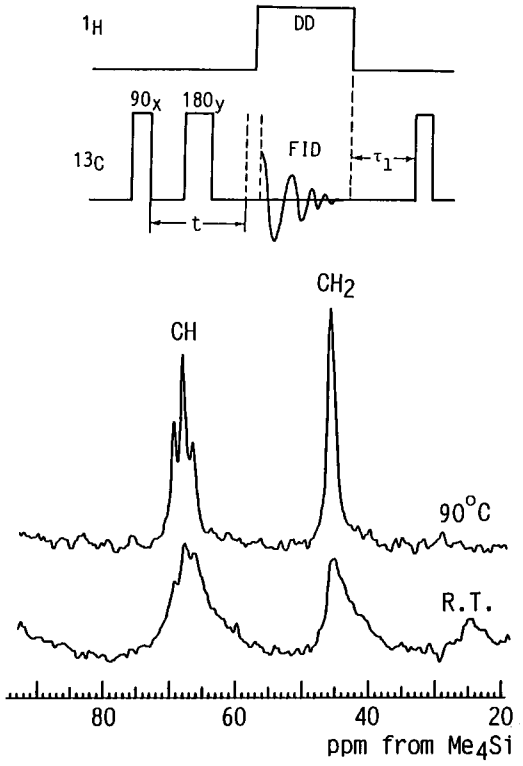

Figure 10 Spectrum of the rubbery component in A-PVA with a water content of 18%, which was measured by the pulse sequence shown at the top of the figure

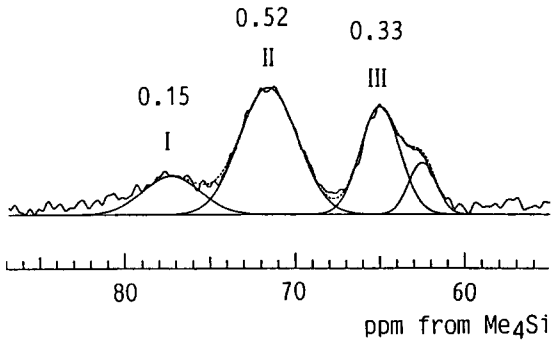

Figure 11 Lineshape analysis for the CH line of the crystalline component of A-PVA with a water content of 18%. The broken line is the composite curve of the three components shown by solid lines and the numerical values are the fractions of lines I, II and III which were corrected by equation (6)

with those associated with intramolecular and intermolecular hydrogen bonding. Therefore, such a component free from hydrogen bonds may be detected as an upfield component of line III, probably as a result of the enhancement in resolution by water. A similar component was also observed for the crystalline components of PVA fibres with different draw ratios and the fractions tended to increase with increasing draw ratio[25].

In *Figure 11* the integrated fractions of lines I, II and III are also shown, which were obtained by lineshape analysis and corrected by equation (6) using T_{1C} values shown in *Table 5*. Interestingly, the fractions of lines I and II significantly increase compared to those for the dry sample. This may suggest that the probability of intramolecular hydrogen bonding is increased upon addition of water. Similar increases in fractions of lines I and II were also found for the crystalline component of the dry PVA sample at higher temperatures[24]. More detailed discussion will be given in a future publication after completion of this work.

REFERENCES

1 Imai, K., Ukita, J. and Matsumoto, S. *Kobunshi Kagaku* 1959, **16**, 597
2 Zhurkov, S. N. and Levin, Y. *Dokl. Akad. Nauk, SSSR* 1949, **67**, 87
3 Glatt, L. and Ellis, J. W. *J. Chem. Phys.* 1951, **19**, 449
4 Akahane, T., Kazusa, Y. and Nakayasu, H. *Kobunshi Ronbunshu* 1980, **37**, 383
5 Komorski, R. A. (Ed.), 'High Resolution NMR Spectroscopy of Synthetic Polymers in Bulk', VCH, Dearfield Beach, 1986
6 Kitamaru, R., Horii, F. and Murayama, K. *Macromolecules* 1986, **9**, 636
7 Nakagawa, M., Horii, F. and Kitamaru, R. *Polymer* 1990, **31**, 323
8 Saito, S., Moteki, Y., Nakagawa, M., Horii, F. and Kitamaru, R. *Macromolecules* 1990, **23**, 3256
9 Hirai, A., Horii, F., Kitamaru, R., Fatou, J. G. and Bello, A. *Macromolecules* 1990, **23**, 2913
10 Horii, F., Hirai, A., Kitamaru, R. and Sakurada, I. *Cellulose Chem. Technol.* 1985, **19**, 513
11 Horii, F., Hirai, A. and Kitamaru, R. *Macromolecules* 1986, **19**, 930
12 Horii, F. in 'Nuclear Magnetic Resonance in Agriculture' (Eds P. E. Pfeffer and W. V. Gerasimowicz), CRC Press, Florida, 1989, Ch. 10
13 Horii, F., Hirai, A., Yamamoto, H. and Kitamaru, R. in 'Cellulose: Structural and Functional Aspects' (Eds J. F. Kennedy, G. O. Phillips and P. A. William), Ellis Horwood, Chichester, 1990, p. 125
14 Terao, T., Maeda, S. and Saika, A. *Macromolecules* 1983, **16**, 1535
15 Horii, F., Ito, T. and Kitamaru, R. *ACS Polym. Prepr.* 1988, **29**(1), 27
16 Matsuzawa, S., Yamaura, K., Noguchi, H. and Hayashi, H. *Makromol. Chem.* 1973, **165**, 217
17 Murahashi, S., Yuki, H., Sano, T., Yonemura, U., Tadokoro, H. and Chatani, Y. *J. Polym. Sci.* 1962, **62**, S77
18 Inoue, Y., Chujo, R., Nishioka, A., Nozakura, S. and Iimuro, H. *Polym. J.* 1973, **4**, 244
19 Wu, T. K. and Sheer, M. L. *Macromolecules* 1977, **10**, 529
20 Bunn, C. W. *Nature* 1948, **4102**, 929
21 Sakurada, I., Futino, K. and Okada. *Bull. Inst. Chem. Res., Kyoto Univ.* 1950, **23**, 78
22 Imashiro, F., Maeda, S., Takegoshi, K., Terao, T. and Saika, A. *Chem. Phys. Lett.* 1983, **99**, 189
23 Ketels, H., Hean, J., Aerdts, A. and Velden, G. *Polymer* 1990, **31**, 1419
24 Hu, S., Horii, F., Odani, H., Matsuzawa, S. and Yamaura, K. *Polym. Prepr., Japan* 1989, **38**, 3296
25 Hu, S., Horii, F., Odani, H., Narukawa, H. and Kajitani, K. *Polym. Prepr., Japan* 1990, **39**, 1098
26 McArthur, D. A., Hahn, E. D. and Walstedt, R. E. *Phys. Rev.* 1969, **188**, 609
27 Mehring, M. 'Principles of High Resolution NMR in Solids', 2nd Edn, Springer-Verlag, Berlin, 1983, p. 151
28 Stejskal, E. O., Schaefer, J. and Stager, T. R. *Faraday Symp. Chem. Soc.* 1979, **13**, 56
29 Horii, F., Hirai, A. and Kitamaru, R. *J. Carbohydr. Chem.* 1984, **3**, 641
30 Torchia, D. A. *J. Magn. Reson.* 1981, **44**, 117
31 Sakurada, I. 'Polyvinyl Alcohol Fibres', Marcel Dekker, New York and Basel, 1985, p. 115
32 Kikukawa, K., Nozakura, S. and Murahashi, S. *Kobunshi Kagaku* 1968, **25**, 19
33 Horii, F., Hu, S., Ito, T., Odani, H., Kitamaru, R., Matsuzawa, S. and Yamaura, K. *Polym. Prepr., Japan* 1988, **37**, 2602
34 Hu, S., Horii, F. and Odani, H. *Bull. Inst. Chem. Res., Kyoto Univ.* 1991, **69**, 165